Mechanism of Dissolution-Induced Nanoparticle Formation from a Copovidone-Based Amorphous Solid Dispersion

Paul Harmon,*,† Kendra Galipeau,† Wei Xu,‡ Chad Brown,‡ and W. Peter Wuelfing†

†Analytical Sciences, Merck Research Laboratories, Merck & Co., Inc., West Point, Pennsylvania 19486, United States
‡Formulation Sciences, Merck Research Laboratories, Merck & Co., Inc., West Point, Pennsylvania 19486, United States

S *Supporting Information*

ABSTRACT: Amorphous solid dispersions (ASDs) have been increasingly used to maximize human exposures from poorly soluble drug candidates. One well-studied advantage of ASDs is the increased amorphous drug solubility compared to crystalline forms. This provides more rapid dissolution rates. An additional advantage of ASDs is that the dissolution process of the ASD particle may also rapidly transform much of the drug present in the ASD particle to small (<1 μm) amorphous drug nanoparticles which will have fast dissolution rates. This work examines the mechanism by which this nanoparticle formation occurs by studying an ASD consisting of 70−80% copovidone, 20% anacetrapib (a low solubility lipophilic drug), and 0−10% TPGS (D-α-tocopheryl polyethylene glycol 1000 succinate, a surfactant). Nanoparticle formation is found to derive from a rapid amorphous drug domain formation *within the ASD particle,* driven by copovidone dissolution from the particle. The role of surfactant in the ASD particle is to prevent an otherwise rapid, local drug domain aggregation event, which we term "hydrophobic capture". Surfactant thus allows the amorphous drug domains to escape hydrophobic capture and diffuse to bulk solution, where they are reported as nanoparticles. This view of surfactant and nanoparticle formation is compared to the prevailing view in the literature. The work here clarifies the different roles that surfactant might play in increasing nanoparticle yields and extending the useful drug loading ranges in copovidone-based ASDs.

KEYWORDS: *solid dispersion, nanoparticles, solubility, dissolution, surfactant, hydrophobic capture, scaffold particle*
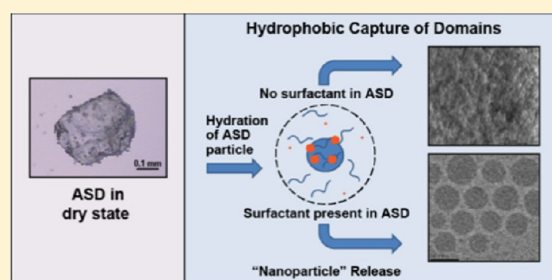
INTRODUCTION

The pharmaceutical literature has many examples of methods to mitigate solubility limitations of compounds. These include crystalline nanoparticles, emulsifying drug delivery systems, surfactants, cosolvent systems, and salts.[1−5] Poorly soluble compounds continue to enter developmental pipelines and have remained a challenge. In the past two decades amorphous solid dispersions (ASDs), made by either spray drying (SD) or hot melt extrusion (HME), have been intensely studied and developed as potentially viable commercial processes.[6−12] In these processes poorly soluble drug is dispersed in a matrix of a water-soluble polymer (and potentially a surfactant). Use of polymers such as copovidone and HPMCAS in ASDs thus enables both solubility and concomitant dissolution rate advantages. While the solubility advantages of amorphous versus crystalline drug have been well-described in the literature, some of the mechanistic details of the dissolution process of the ASD particles are still being actively investigated.[13−21]

One of the unique properties of the dissolution process of some ASDs is the phenomenon where drug concentrations in aqueous media, as measured by 1 μm filtration or gently centrifuged samples, are significantly larger than the known amorphous drug solubility (the molecularly dissolved drug).[6,14−20] These novel studies utilized dynamic light scattering (DLS), filtration, membrane permeability, and field flow fractionation to characterize the dissolution products of the amorphous dispersions. The solubility values above the amorphous solubility limit have been termed "apparent solubility", and in these studies investigators show convincingly that the apparent solubility values derive from the extra contributions to total solubility from an amorphous drug nanoparticle phase (perhaps containing minor amounts of polymer or surfactant associated). These papers collectively demonstrate that amorphous nanoparticles can be formed from a variety of drug compounds; nanoparticles are generally <500 nm, and suspensions of the nanoparticles provide drug diffusion rates in dual chamber flux experiments (through Caco-2 cells or low molecular weight filters) that were similar to the molecularly dissolved drug at the amorphous solubility limit. Implicit in the context of this latter finding is that amorphous drug nanoparticles offer rapid dissolution rates as described by simple Noyes−Whitney type mass transfer models[8] which can resupply molecularly dissolved drug to solution in the presence of absorption. Such size reduction by the ASD dissolution

process thus offers an additional route of ASD enhancement to dissolution rate.

While their presence and potential impact on drug absorption have been characterized, a mechanistic view of "how and where" nanoparticles are actually formed from ASDs has not been definitively described. Taylor et al.[14] has considered this question in some detail in copovidone and hydroxpropyl methylcellulose based dispersions of both felodipine and indomethacin. The authors speculated that, at lower drug loadings, almost all the drug present in the ASD particle is able to transiently solubilize to form a highly supersaturated solution "local" to the dissolving ASD particle. In this construct, sub-micrometer amorphous drug particles derive from a precipitation type event from this highly supersaturated solution. Indeed, this latter type of solution-based mechanism of nanoparticle formation from ASDs is often implied.[6,12,16]

Herein we present experimental data aimed at understanding how this "local" amorphous drug nanoparticle formation occurs when ASD particles are placed into water. In Merck's developmental efforts around poorly soluble compounds, we realized that anacetrapib (Figure 1, upper) in a copovidone
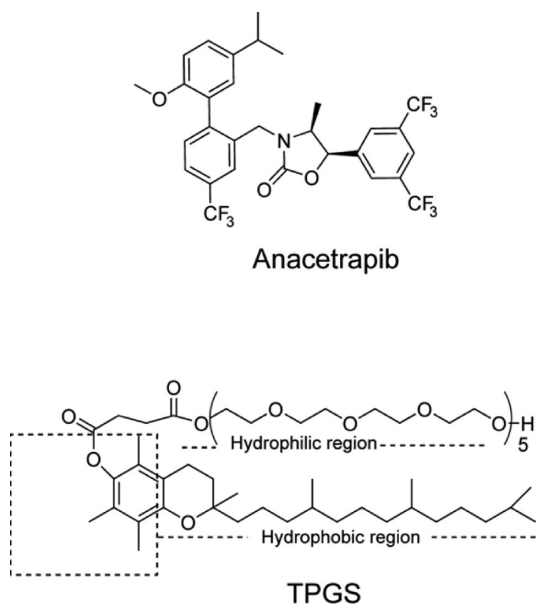

Figure 1. Upper, structure of anacetrapib. Anacetrapib has no pK_a or pK_b, log P = 8.8, and water solubility is less than 0.1 μg/mL. Lower, structure of amphiphilic TPGS, which has over 200 mg/mL water solubility. Dashed square is 7.7 Å on each side (60 Å^2) shown to scale with the TPGS bond lengths and corresponds to the closest packed TPGS monolayer footprint (details in text).

polymer system offered an ideal ASD system to examine this fundamental question. Anacetrapib is a poorly soluble, lipophilic drug substance which has negligible propensity to crystallize from aqueous solution. High yields of sub-micrometer amorphous drug particles may be obtained from copovidone-based ASD particles which contain appropriate surfactant. Thus, in this work we study amorphous nanoparticle evolution from copovidone-based ASD particles in which the anacetrapib drug loading is kept constant at 20%, but in which the surfactant weight percent ranges from 0% to 10%. The surfactant used is TPGS (D-α-tocopheryl polyethylene glycol 1000 succinate, Figure 1 lower), and the ASD particles are

made by the HME process. The appearance of copovidone, TPGS, and anacetrapib nanoparticles coming into the bulk solution is monitored every 15 s over the first few minutes upon contact with water (and then over the next 2 h). These data, along with optical images of the HME particle hydration, and DLS measurements of the nanoparticles formed (as a function of TPGS level in the HME particle) provide for a novel understanding of nanoparticle evolution in this system. The key finding is that nanoparticle creation is best described as an amorphous phase-separation event of the anacetrapib, which is driven by rapid copovidone diffusion out of the HME particle. Thus, nanoparticle formation occurs rapidly *within* each HME particle. The potential generality of these observations to other copovidone/drug and PVP/drug ASDs is discussed, and the important role of surfactant in nano-particle release is revealed.

MATERIALS AND METHODS

Materials. Anacetrapib was obtained from Merck & Co., Inc. (Rahway, NJ). TPGS was purchased from Isochem (Vert-Le-Petit, France). Copovidone (Kollidon VA 64) was purchased from BASF (Ludwigshafen, Germany). Acetonitrile and HPLC grade water were obtained from Fisher Scientific (Fair Lawn, NJ). Sodium dodecyl sulfate was purchased from ACROS (NJ). The 1 μm filters (APFB) used were obtained from Millipore (Billerica, MA). Avicel (microcrystalline cellulose, PH 101) used to dry mix with HME powders to help wet and disperse the HME powders was obtained from FMC (Philadelphia, PA).

Preparation of HME Formulations of Anacetrapib. Anacetrapib has a melting point of approximately 72 °C and is chemically stable at elevated temperatures. Formulations of anacetrapib were extrusion compounded at a 20% w/w drug load with varying copovidone and TPGS levels (Table 1). The

Table 1. Primary HME Compositions Studied in This Work[a]

nomenclature used for HME composition	composition (wt %)			surface/drug ratio (wt %)
	copovidone	anacetrapib	TPGS	
0%	80	20	0.0	NA
1%	79	20	1.0	5
2%	78	20	2.0	10
3.5%	76.5	20	3.5	18
5%	75	20	5.0	25
7.2%	72.8	20	7.2	36
10%	70	20	10.0	50

[a]HME designations used correspond to the weight % TPGS in the HME.

extrusion was carried out with a corotating 7.5 mm twin screw extruder with L/D = 15 and 1 mm × 10 mm slit die (MP&R, Hackensack, NJ). Copovidone and TPGS were pregranulated at a 15% w/w concentration of TPGS. Approximately 10.0 g of each composition was prepared by preblending the pregranulated copovidone/TPGS with copovidone and anacetrapib in a turbula blender for 10 min prior to extrusion to help ensure compositional homogeneity. The extruder was equipped with 3 mixing paddles offset by 30° and was heated to provide a target product temperature of 160 °C, and the screw speed was set at 100 rpm. Strands of clear, glassy extrudate were quenched with a Vortec cold air gun (AiRTX, Cincinnati, OH). Extrudates of each composition were dry milled in a Polymix PX-MFC 90D

mill (Kinematica AG, Luzern, Switzerland) equipped with hammer blades and a 500 μm screen at 3500 rpm. The mean PSDs after milling were about 100 μm.

Cryogenic Transmission Electron Microscopy (Cryo-TEM). A nanoparticle suspension was prepared using the 10% TPGS HME composition shown in Table 1, at 2 mg/mL anacetrapib. The HME powder was stirred in deionized water for approximately 15 min. Five microliters of solution was deposited on a 200 mesh copper grid covered with Quantifoil holey carbon foil (Quantifoil Micro Tools GmBH, Jena, Germany). A thin aqueous film (ca. 100 nm thick) of the nanoparticle suspension was formed by blotting and then was rapidly vitrified by plunging it into liquid ethane using the FEI Vitrobot freeze plunger. The grid with the vitrified thin film was transferred into the microscope chamber of an FEI Tecnai T12 Bio-Twin TEM transmission electron microscope (Philips, Eindhoven, NL) operating at 120 kV. The specimen temperature was set at −170 °C to −180 °C, and low-dose imaging conditions were used. Images were recorded using a Gatan Ultrascan 1000 CCD Camera.

Transmission Electron Microscopy (TEM) with Negative Staining. A nanoparticle suspension was prepared using the 0% TPGS HME composition shown in Table 1, at 0.1 mg/mL anacetrapib. The HME powder was stirred in deionized water for approximately 20 min. A 1% aqueous uranyl acetate stain was prepared, and a 300 mesh carbon coated copper grid was glow discharged (Electron Microscopy Sciences, Hatfield, PA). Ten microliters of solution was deposited on the shiny side of the grids for ~1 min. Filter paper was used to wick off excess sample. Ten microliters of uranyl acetate was deposited on the grid for ~30 s before excess was wicked away with filter paper. The grids were air-dried prior to being transferred into the microscope chamber of an FEI Tecnai T12 Bio-Twin TEM transmission electron microscope (Philips, Eindhoven, NL) operating at 120 kV. Images were recorded using a Gatan Orius SC 1000 CCD. All solids imaged were amorphous by TEM; no Bragg spots were detected by Fourier transform.

Particle Size Analysis. The particle size distribution of the HME samples after addition to water was determined by dynamic light scattering (DLS) using a Malvern Zetasizer Nano-ZS (Malvern, U.K.). Transmission values of 0.3−10% nominal (attenuator = 6−9) were recorded. The attenuator values varied depending on % nanoparticle yield.

Optical Microscopy of HME Particles in Contact with Water. Hydration images were collected with an Olympus BX51 with 20× objective using QCapture Pro v. 6.0 software. Approximately 20 mg of HME ASDs was spread on a glass slide. A thin layer of silicone grease was spread on three edges of a glass coverslip to form a seal to contain the water. An image was captured in the dry state; subsequently ~50 μL of deionized water was placed at the open edge of the coverslip and allowed to wick between the two pieces of glass. Hydrated images were captured as soon as the water front encountered the HME particle and approximately every 15 s thereafter.

Powder X-ray Diffraction (PXRD), Thermal Analysis, and Optical Microscopy of Milled HME Powders and Nanoparticles. PXRD measurements on HME samples were collected on a Panalytical X'pert Pro diffractometer with Cu Kα1 radiation of of 1.5406 Å in the transmission mode to check for crystallinity of the drug. The samples were scanned between a two theta range of 2 and 40° at a step size of 0.0167° for 1 h at ambient conditions. The tube power setting was 45 kV and 40 mA. Differential scanning calorimetry was performed on a

TA Instruments Q-1000 modulated DSC to evaluate the thermal behavior of the HME samples. Samples were initially cooled to −20 °C for 5 min and then heated to 130 °C at 2 °C/min. Optical microscopy was collected with a Nikon Eclipse with 20× objective. Cross-polarizers were used to confirm the amorphous state of ASD formulations (lack of birefringence) after wetting with immersion oil.

Scanning Electron Microscopy (SEM). The 0% TPGS HME milled particles were examined before and after hydration in water by field emission scanning electron microscopy (QUANTA FEG 250). SEM images were taken at an accelerating voltage of 5 kV at 40000× magnification.

HPLC Analysis of Anacetrapib, Copovidone, and TPGS. Anacetrapib was analyzed by HPLC with UV detection at 210 nm. Isocratic elution was used with 85/15 acetonitrile/water, flow 1.0 mL/min and a 5 cm Waters Symmetry C18 column (3.5 μm silica) at 30 °C. Anacetrapib eluted in approximately 3 min. TPGS was not eluted under these conditions, but was eluted in a 100% acetonitrile wash at the end of the sample run. TPGS quantitation was done similarly by HPLC, with 210 nm detection using a Waters X Bridge C18 column (5 cm, 3.5 μm silica) at 30 °C with acetonitrile as the mobile phase. TPGS elutes in approximately 4 min under these conditions. Copovidone was also monitored by HPLC with UV detection at 210 nm with the same Waters Symmetry C18 column described above. Copovidone was intentionally eluted very near the void volume with an isocratic mobile phase of 50/50 acetonitrile/water to keep the copovidone peak as narrow as possible. Samples from dissolution experiments in water were diluted 1:1 in acetonitrile to match the mobile phase conditions thus minimizing void volume artifacts. Standard areas were examined from 50 to 150% of the nominal copovidone concentration and found to show acceptable linearity and a Y-intercept near zero. After copovidone analysis, both anacetrapib and TPGS were eluted with a 100% acetonitrile mobile phase. Quantitation of all components was made against gravimetrically prepared standards.

ASD Dissolution Experiments. Typical sample preparation for an ASD dissolution experiment involved weighing ~50 mg of milled HME strand (a powder) to a scintillation vial, to which approximately 100 mg of microcrystalline cellulose was added and dry mixed. This helped provide uniform wetting and dispersion of the HME particles when poured into the 100 mL of stirring HPLC grade water (150 rpm, 0.8 in. stir bar, 100 mL glass bottle). Experiments were carried out at controlled room temperature (~23.5 °C ± 1.5 °C). Sample clarification for "apparent solubility" values was obtained by filtering the ASD containing solutions through a 1 μm glass filter. This filtration thus allowed passage of all anacetrapib nanoparticles formed, as well as all molecularly dissolved drug, copovidone, and TPGS. Approximately 5 mL of volume per time point was taken; the first 2 mL was discarded, and the remaining 3 mL of sample was placed in a test tube. The filtrates were injected neat for TPGS analysis, diluted 1:1 with acetonitrile for copovidone analysis, and diluted 1:10 with acetonitrile for anacetrapib analysis. Ultracentrifugation (Optima TLX ultracentrifuge, TLA 110 rotor, 10 min @ 348000g (rmax)) was also used to remove nanoparticles to measure molecularly dissolved anacetrapib.

TPGS Association with Nanoparticles and Competitive Displacement with SLS. Displacement of TPGS from nanoparticles by SLS was determined by carrying out the ASD dissolution experiment as described above, with a nominal target concentration of 100 μg/mL TPGS, and allowing the

usual nanoparticle evolution to occur. An additional 1 h of stirring is given to ensure that TPGS is equilibrated between the bulk solution and the nanoparticles. The samples were then diluted 1:1 into dilute SLS solutions in water to give final SLS concentrations from 0.0 mg/mL SLS (control sample) to 1.0 mg/mL SLS. The nanoparticle suspensions were allowed to equilibrate with the SLS for 90 min, and the TPGS concentration was again measured both pre- and post-ultracentrifugation. (Note that the SLS concentration remained below its CMC in water, and less than 0.5% of the total anacetrapib was actually molecularly dissolved at the highest SLS concentration used.)

■ RESULTS

Thermal and XRD Analysis of Extrudates. No evidence of anacetrapib crystallinity was observed in any extrudate materials either by thermal, XRD, or optical microscopy. The materials appear homogeneously mixed and amorphous. Similarly, anacetrapib nanoparticles formed during the dissolution process were also found to be amorphous.

Rate and Extent of Anacetrapib Nanoparticle Appearance into Bulk Solution. Table 1 shows the seven HME ASD compositions containing anacetrapib examined in this work. Figure 2 shows the μg/mL anacetrapib found in the 1 μm
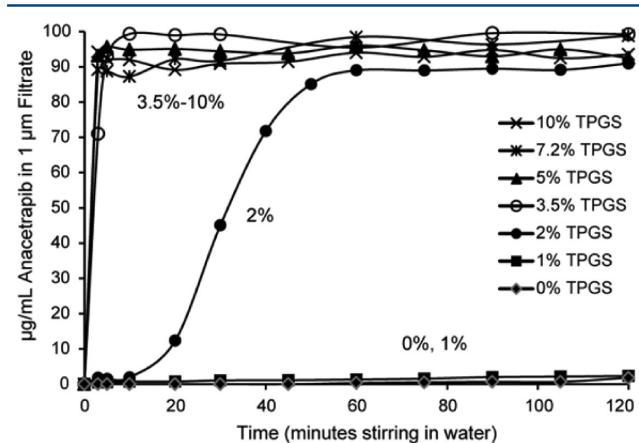

Figure 2. One micrometer filtrate data for 100 μg/mL anacetrapib added to water (23 °C, 0−2 h) from 10%, 7.2%, 5%, 3.5%, 2%, 1%, and 0% TPGS HME (post 1 μm filtered, room temperature). Ultracentrifuged data all shows anacetrapib at the amorphous solubility limit (<1 μg/mL) and is omitted for clarity. Y-axis values derive from anacetrapib nanoparticles.

filtrate for 100 μg/mL target anacetrapib concentrations of all seven HME compositions in Table 1 added to water at 23 °C (as described in Materials and Methods). The molecular solubility of anacetrapib in water is below 0.1 μg/mL, and ultracentrifugation of any samples in Figure 2 yields anacetrapib solubility values consistent with the true molecular solubility value. Thus, in Figure 2, the anacetrapib Y-axis values are completely dominated by anacetrapib nanoparticles which readily pass through the 1 μm filters. Note the wide range of behaviors as a function of the TPGS content in the HME particle. The 3.5%, 5%, 7.2%, and 10% TPGS samples rapidly provide close to 90 μg/mL anacetrapib nanoparticles within 3− 5 min. The 2% TPGS composition shows much slower nanoparticle evolution, with significant apparent solubility developing over the 20−60 min time frame. On the other hand the 0% and 1% TPGS HME produce a maximum of only

$\sim$2 μg/mL nanoparticles even by the end of 2 h of stirring in water at 23 °C.

Monitoring Copovidone, TPGS, and Anacetrapib Nanoparticle Release to Bulk Solution. Given the data in Figure 2 we wanted to understand in more detail the first 5 min of the experiment, where nanoparticle yields increase from zero to over 90% in the 3.5%, 5%, 7.2%, and 10% TPGS compositions. To further probe the system, the copovidone, TPGS, and anacetrapib nanoparticles were all monitored as they appear in the 1 μm filtrates. Figure 3 (upper) isolates the
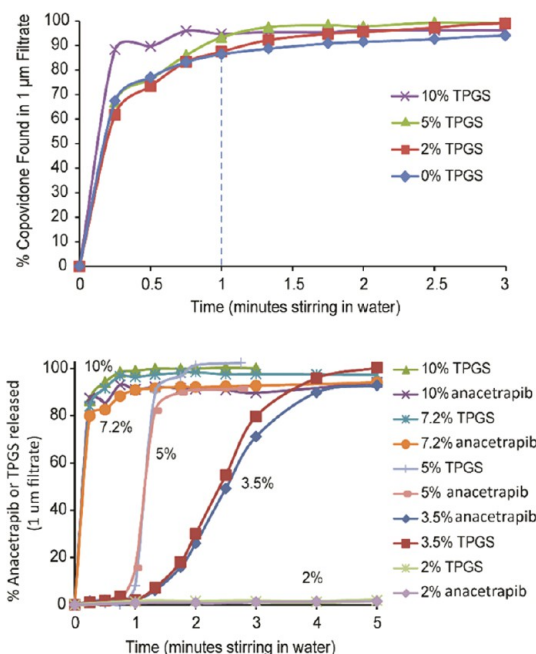

Figure 3. Upper, copovidone release into bulk solution over 0−3 min for the 0%, 2.0%, 5%, and 10% TPGS HME cases. Copovidone is 85− 95% dissolved into bulk solution in 60 s. Lower, TPGS and anacetrapib nanoparticle release into bulk solution (0−5 min) for the 2%, 3.5%, 5%, 7.2%, and 10% TPGS HME formulations. Note that TPGS and anaceptrapib profiles are nearly identical.

copovidone release to bulk solution data at 15 s intervals over the first 3.0 min of the experiment in Figure 2. The copovidone data for the 0%, 2%, 5%, and 10% TPGS HME extrudates are shown and bracket the 1.0%, 3.5%, and 7.2% TPGS HME data (omitted for clarity). The copovidone in all four cases rapidly diffuses into the bulk solution, reaching ca. 90% of the nominal concentration added within about 60 s.

The lower portion of Figure 3 shows the anacetrapib nanoparticle appearance as well as the appearance of TPGS over the first 5 min of the experiment. The 2%, 3.5%, 5%, 7.2%, and 10% TPGS HME compositions are shown (TPGS and anacetrapib data for each, 10 data curves). The 7.2% and 10% HME data show that in both cases the TPGS and anacetrapib nanoparticles diffuse into bulk solution very quickly and appear at similar rates to the copovidone release profiles (Figure 3, upper). However, the 3.5% and 5% HME composition data both show that the TPGS release into bulk solution is delayed (compared to copovidone release) and, in fact, proceeds concomitantly with anacetrapib nanoparticle appearance. In the 5% TPGS HME case the delay is approximately 1 min, while for the 3.5% TPGS case both TPGS and anacetrapib nanoparticles come into bulk solution over the 2−5 min time

frame and appear in strikingly similar proportions. The lower portion of Figure 3 also highlights another fascinating result for the 2% TPGS HME case, in that minimal TPGS (or anacetrapib nanoparticles) diffuses into bulk solution over 5.0 min, despite the copovidone having completely dissolved out of the HME particle.

Figure 4 accounts for the remaining 5 to 120 min of the experiment for the 2% and 1% TPGS HMEs. Again, for the 2%
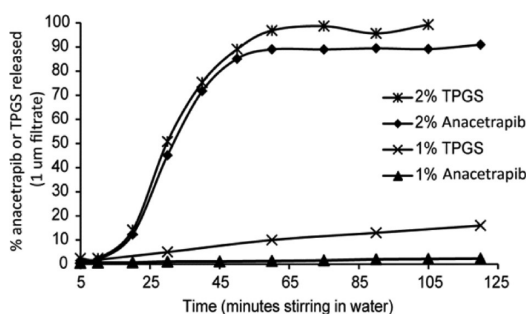

Figure 4. Remaining 5−120 min portion of experiment showing TPGS and anacetrapib nanoparticle release for the 2% and 1% TPGS HME samples. The 2% TPGS HME case again shows simultaneous appearance of anacetrapib nanoparticles and TPGS.

HME composition both TPGS and anacetrapib nanoparticles appear in bulk solution concomitantly, in this case over the 20−50 min time frame. The 1% TPGS composition behaves somewhat differently, in that some TPGS appears to slowly come into bulk solution (about 15% by the end of the 2 h experiment) while less than 2% of the anacetrapib is measurable in the 1 μm filtrate (as shown in Figure 2).

DLS Measurements of the Nanoparticle Size Distributions and Cryo-TEM. Figure 5 shows representative
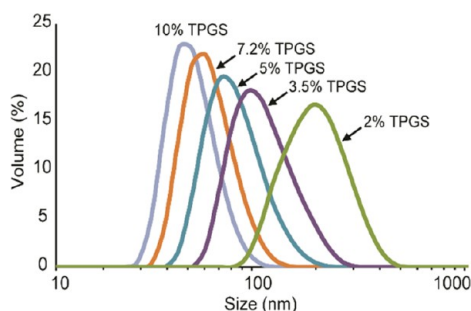

Figure 5. PSD distributions measured for nanoparticles spontaneously released to bulk solution at 23 °C. Data shown is after 1 h stirring in water. Labeling refers to the % TPGS in the extrudate (Table 1).

nanoparticle size distributions measured by DLS after full evolution of nanoparticle release to bulk solution (once released, nanoparticle sizes in bulk solution are stable throughout the 2 h experiment). There is a clear trend of decreasing nanoparticle sizes evolved with increasing levels of TPGS in the extrudate. Table S1 lists D_{50} values (volume distribution based) and their associated PSD width parameters. The determined particle size range is ∼50 nm to ∼200 nm, depending on level of TPGS in the HME particle. These trends are rationalized below.

Cryo-TEM imaging was undertaken to examine the 10% TPGS HME nanoparticles released to the bulk solution (as a representative case). Figure 6 shows the cryo-TEM obtained
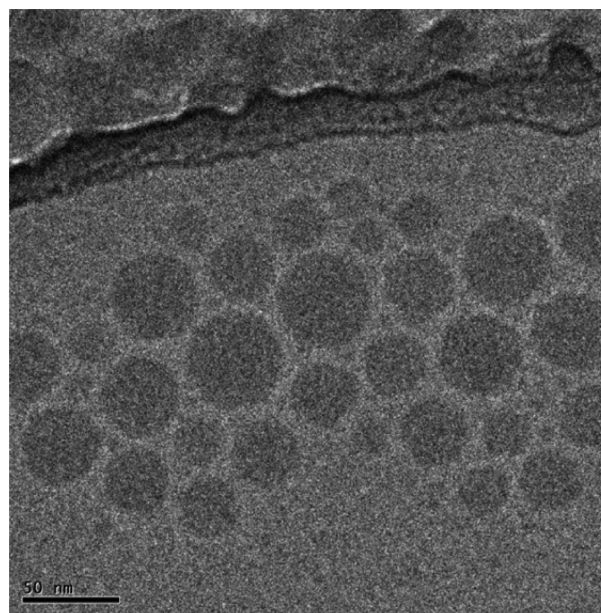

Figure 6. Cryo-TEM of nanoparticle suspension from 10% TPGS HME. Edge of holey carbon film opening appears in the upper portion of the figure. Nanoparticles collect in the ca. 100 nm thick water film near the edge of the hole. Note regular spacing between particles.

approximately 20 min after the dry milled HME powder was added to water. The 3 μm holey carbon support film used (see Materials and Methods) produces a water film that is only ca. 100 nm thick,[22,23,23−25] and often nanostructures are concentrated and pack closely together near the edges of the holey carbon film (seen in the upper part of the image in Figure 6). The anacetrapib nanoparticles are spherical, well-defined structures the sizes of which are consistent with the DLS data in Figure 5 for the 10% TPGS HME. Note that in Figure 6 there is a consistent "spacing" of 6−8 nm between the nanoparticles preventing contact of the most electron dense parts of the nanoparticles. This is interesting in that contact between neighboring "naked" nanoparticles can be expected[22−25] under these conditions. We hypothesize that this spacing is occupied by associated TPGS molecules (this is discussed in more detail in the context of Figure 10 below).

Optical Images of the HME Particles Placed in Contact with Water. The data in Figures 2−4 gave us pause to reflect carefully on visual observations. The 5%, 7.2%, and 10% TPGS HME particles can be seen at first but disappear visually within 1 to 2 min. When the 2% TPGS HME particles are placed into water, particles visually persist for over 20 min, and then disappear over the next 20 min, concurrent with nanoparticles appearing in solution (Figure 2, Figure 4). The 0 and 1% TPGS HME particles remain visible to the eye throughout the 2 h experiment.

These visual observations prompted us to take optical images as these ca. 100 μm milled HME particles come into contact with a gently moving water front under a microscope slide (as described in Materials and Methods). Figure 7a−f shows the 0% TPGS composition. Upon first contact with water, the HME particle edges appear to soften (appear less distinct) and a water front can be seen rapidly progressing through the particle from exterior surfaces toward the particle center. The kinetics of the copovidone appearance in bulk (Figure 3, upper) correlate well with the water front progression in Figure 7
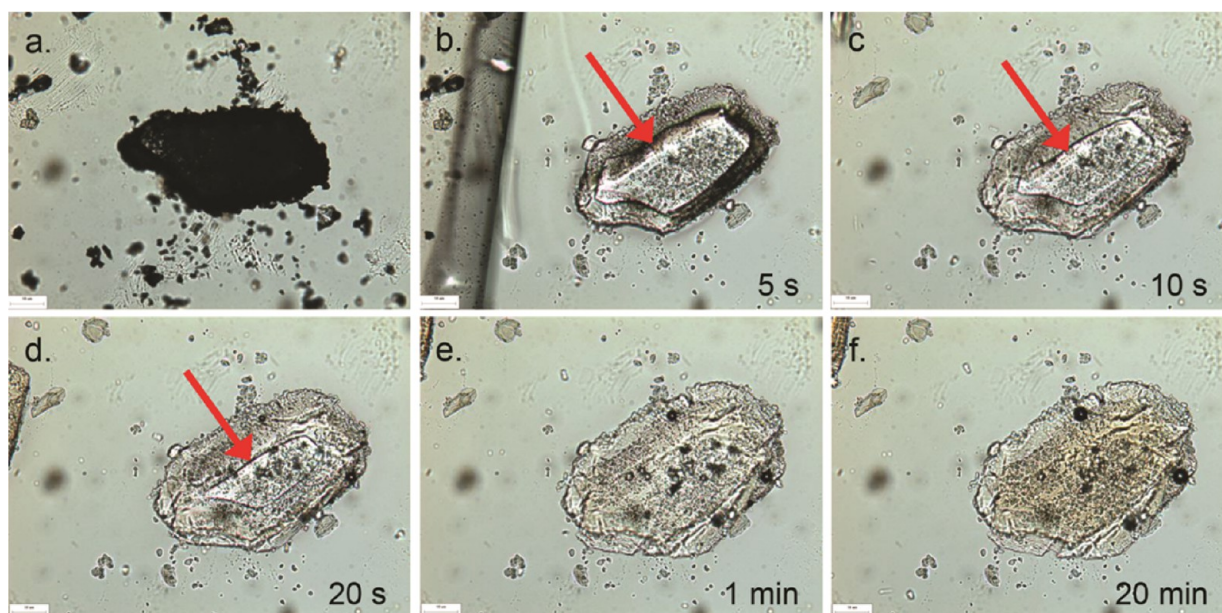
Figure 7. (a–f) Optical microscopy images of 0% TPGS:80% copovidone:20% anacetrapib taken at 20× magnification. Scale bar for all 6 images is 10 μm. The red arrow indicates the progression of the water front as it hydrates the particle. (a) Dry HME particle. (b) HME particle 5 s after water front passes over particle, moving from right to left. (c) HME particle 10 s after hydration. (d) HME particle 20 s after hydration. (e) HME particle 1 min after hydration. The particle is fully hydrated by 1 min, and over 90% of copovidone has diffused out of particle. (f) HME particle 20 min after hydration. No further changes to the particle could be observed.
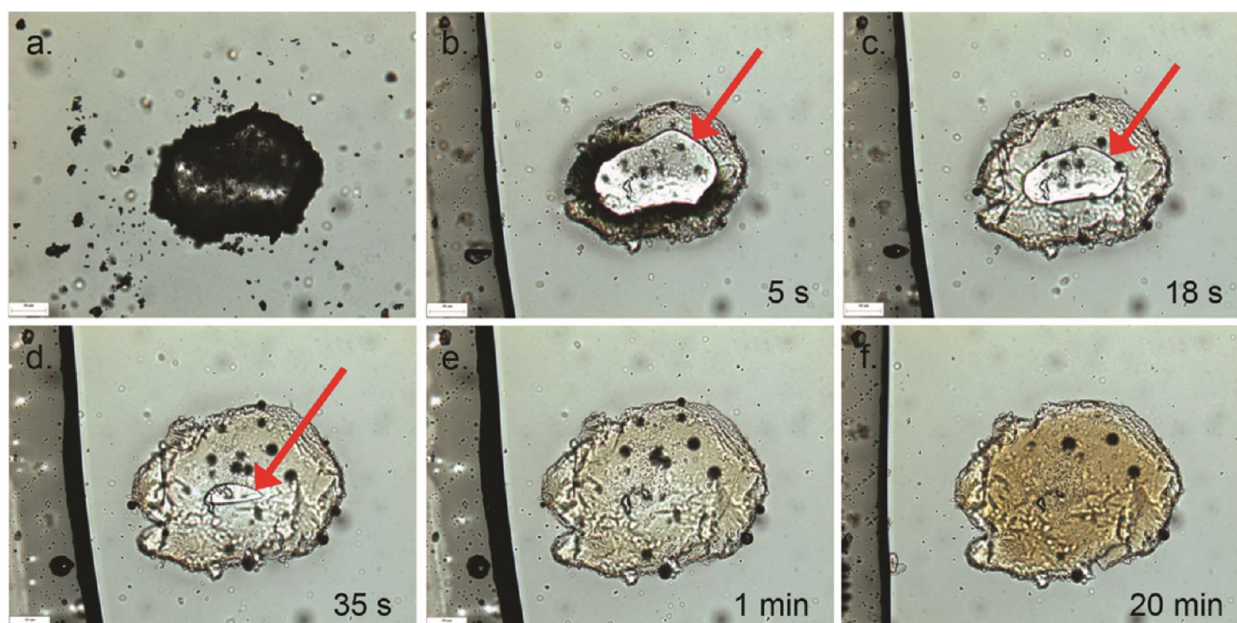

Figure 8. (a–f) Optical microscopy images of 2% TPGS:78% copovidone:20% anacetrapib taken at 20× magnification. Scale bar for all 6 images is 10 μm. The red arrow indicates the progression of the water front as it hydrates the particle. (a) Dry HME particle. (b) HME particle 5 s after water front passes over particle, moving from right to left. (c) HME particle 18 s after hydration. (d) HME particle 35 s after hydration. A small, unhydrated core is visible in this image. (e) HME particle 1 min after hydration. The particle is fully hydrated by 1 min, and ca. 90% of copovidone has exited the particle. (f) HME particle 20 min after hydration.

suggesting that these visual changes reflect copovidone exit from the hydrated regions. Figure 7 shows that, after copovidone leaves the 0% TPGS HME particle, a "scaffold" particle remains, which can only be composed of amorphous anacetrapib. We use "scaffold" to imply that the 80% by mass copovidone in the particle has been replaced by water, leaving behind the insoluble matrix of amorphous anacetrapib in a form that is still a contiguous structure. This scaffold particle survives

not only the conditions of the microscope slide experiment but also is intact at the end of the 2 h 23 °C stirring experiment in Figure 2. Comparison of earlier and later images shows that this scaffold particle formation overall has resulted in a particle that has expanded by perhaps 20% in diameter, and retains the same shape relative to the original HME milled particle. It should be noted that there is still some residual water flow under the microscope slide as the experiment proceeds, although slower
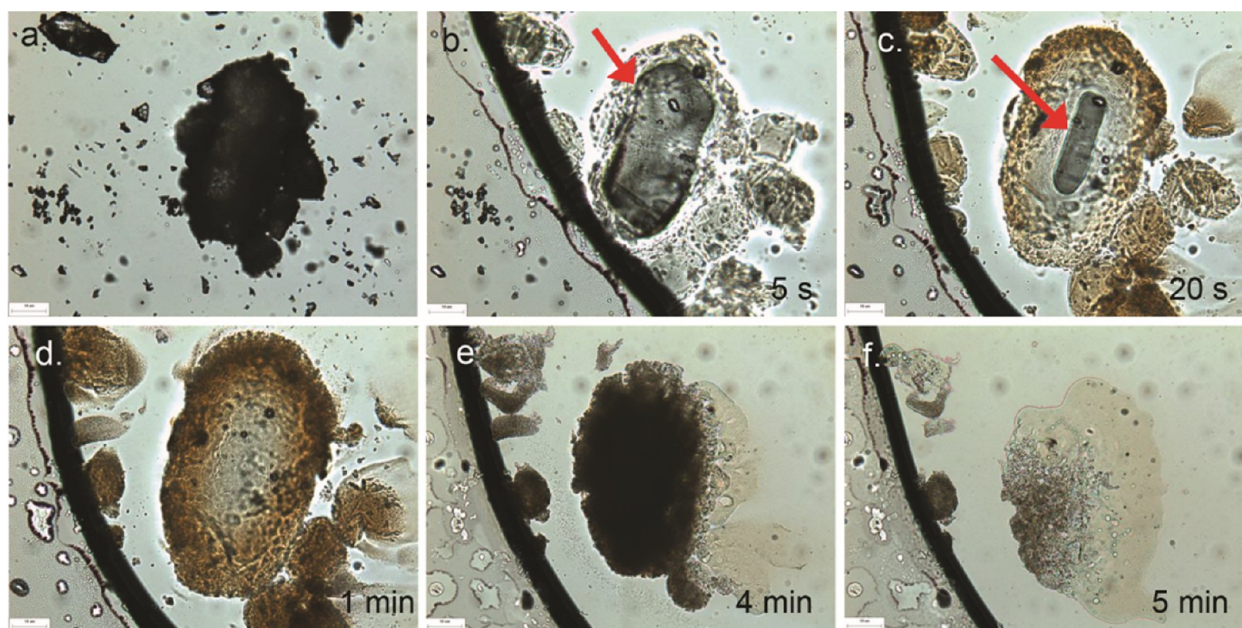
Figure 9. (a−f) Optical microscopy images of 5% TPGS:75% copovidone:20% anacetrapib HME particle taken at 20× magnification. Scale bar for all 6 images is 10 μm. The red arrow indicates the progression of the water front as it hydrates the particle. (a) Dry HME particle. (b) HME particle 5 s after water front passes over particle, moving from right to left. (c) HME particle 20 s after hydration. (d) Fully hydrated HME particle; obvious flow of small anacetrapib particles (right side image) even under the low hydrodynamic forces present between two glass slides. (e) HME particle 4 min after hydration. (f) HME particle 5 min after hydration; most anacetrapib mass has been carried out of the field of view.

than compared to when the water front first passes through the field of vision shown in Figure 7b.

Figure 8a−f shows the optical images for the 2% TPGS HME particle hydration. The 2% TPGS HME particle behaves similarly to the 0% TPGS HME under similar microscopic examination. The same progressive copovidone exit/particle hydration can be seen. There is again a swelling (increase of 20−30% in the scaffold particle diameter) compared to the original HME milled particle size. In this case the scaffold particle seen in the last two images in Figure 8 contains both anacetrapib and >95% of all the initial TPGS (Figure 3, lower). This particle also remains intact throughout the entire microscopic examination (up to 20 min). However, this particle disappears over the 20−50 min time frame under the stirred solution conditions of Figure 2 (along with concomitant appearance of anacetrapib nanoparticles and TPGS into the bulk solution). The 3.5% TPGS particle hydration proceeds similarly to the 2% TPGS particles, forming a similar scaffold particle as that shown in Figure 8. Under stirring conditions this scaffold particle survives only 3−5 min before anacetrapib nanoparticles and TPGS are released.

Figure 9a−f shows the same optical images of the hydration experiment for the 5% TPGS containing particle. The images are similarly arranged. The behavior is similar in terms of rapid water advance to the HME particle core and simultaneous copovidone exit. The scaffold particle again immediately forms right behind the advancing water front. The scaffold particle diameter in the 5% TPGS case is also 20−30% larger than the original HME particle size. In Figure 9d, the copovidone dissolution is nearly complete, and the scaffold particle composition is thus 4 parts anacetrapib and 1 part TPGS by weight (given the composition in Table 1). The 5% TPGS HME scaffold particle is clearly more fragile and is observed to fall apart into much smaller particles even under microscopic slide hydration. After 5 min, Figure 9f shows very little

anacetrapib mass remaining even given the almost static water movement around the particle. In a stirring solution of water, solids forming just behind the advancing water front are more rapidly dispersed than in Figure 9 (Figure 3, 5% HME data implies that, with stirring, solids disperse rapidly just behind the water front).

The 7.2% and 10% TPGS HME particles behave similarly to the 5% TPGS HME particle in the microscope hydration experiment. Even more facile reduction of the original HME mass to small material which diffuses away rapidly is observed. In the stirred solution, there is no evidence of a delay period for the 7.2% and 10% TPGS cases; by the first 15 s time point the copovidone, TPGS, and anacetrapib nanoparticles have all appeared at 80% of target values in the bulk solution (Figure 3, lower).

Disposition of the TPGS Released with Anacetrapib Nanoparticles. The similar rates of appearance of TPGS and anacetrapib nanoparticles into solution in Figures 3 and 4 led us to want to understand if the TPGS was simply surface-associated with the anacetrapib nanoparticles or actually incorporated into the nanoparticles in some manner. TPGS concentrations were measured both pre- and post-ultra-centrifugation (ultracentrifugation removes the nanoparticles and associated TPGS). SLS was used to attempt to competitively displace the TPGS from the anacetrapib nanoparticle surfaces (see Materials and Methods for experimental details). Figure 10 shows that, with no SLS added, there is ~73%, 68%, and 55% of the TPGS associated with the nanoparticles produced from the 2%, 5%, or 10% TPGS HMEs, respectively. However, as SLS is added, the amount of TPGS associated decreases. Nearly 70% of the TPGS that was associated can be displaced by 1.0 mg/mL SLS[26] (Figure 10). Given the very high solubility of TPGS in water, we interpret the SLS effect as competition of SLS and TPGS for the hydrophobic anacetrapib nanoparticle surface.
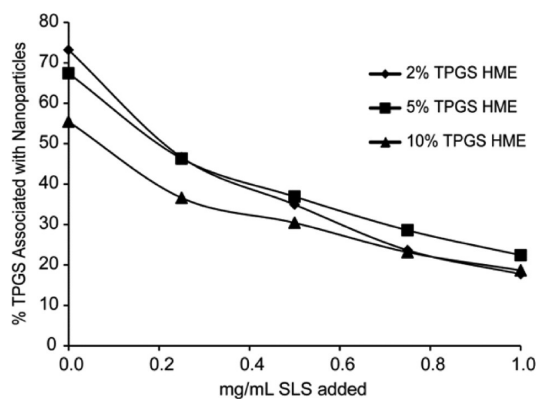
Figure 10. Progressive displacement of the associated TPGS from the 190 nm nanoparticles (2% TPGS HME), 77 nm nanoparticles (5% TPGS HME), and the 48 nm nanoparticle D_{50} PSD (10% TPGS HME).

Table S2 summarizes the 0% and 1% SLS data. The cryo-TEM data (Figure 6, 10% TPGD HME nanoparticles) shows a 6–8 nm spacing between adjacent nanoparticles, which is consistent with the presence of the surface-associated TPGS.[27]

Further Investigation of the 0% HME Scaffold Particle (after Copovidone Exit). Figure 2 illustrates that nanoparticle release from the 0% TPGS HME scaffold particle shown in Figure 7f only represents a few μg/mL anacetrapib. However, if the same 0% TPGS samples (at time points shown in Figure 2) are sonicated for only a few seconds (Crest CP2600 bath sonicator, power setting 8), about 60–70 μg/mL anacetrapib solids pass through the 1 μm filter. The PSD of the sonicated 0% TPGS scaffold particles thus produced is shown by the gray PSD curve in Figure 11. The particles span the 50–500 nm
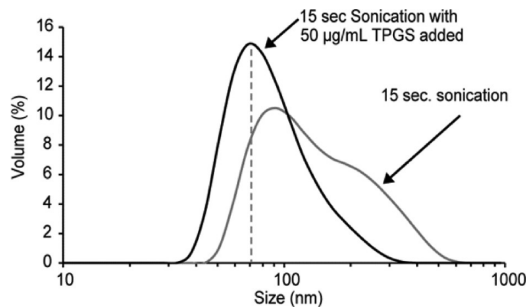

Figure 11. PSD curves for briefly sonicated 0% TPGS samples after 1 μm filtration. Particles represent 60–70% of the anacetrapib mass originally present.

range. If the same experiment is repeated except that 50 μg/mL TPGS is added to the solution just prior to the brief sonication, the resulting PSD shifts even smaller, as shown by the black PSD curve in Figure 11.

Figure 11 argues that the 0% scaffold particle (Figure 7f) should be viewed as deriving from much smaller aggregated amorphous particles. These results prompted us to try to image the hydrated 0% TPGS HME particle with SEM and TEM to look for any nanoscale structures.

Figure 12a–f shows SEM and TEM images of 0% TPGS scaffold particles as described in the Figure 12 caption. The images of the sub-micrometer pieces of 0% TPGS scaffold particles in Figure 12e,f show a remarkable porous, yet connected, structure of the amorphous anacetrapib. This type

of structure must exist throughout the 50–100 μm intact 0% TPGS scaffold particles (as shown in Figure 7e,f). This extended porous structure is consistent with Figure 11: a high fraction of scaffold particle mass converted to sub-micrometer anacetrapib "nanoparticles" with a broad PSD, liberated by simple sonication of the 0% scaffold particles. The anacetrapib solids are amorphous by TEM and XRD.

■ DISCUSSION

Rapid Phase Separation and "Hydrophobic Capture" in the 0% TPGS HME Particle. As described in Results and seen in the images in Figure 7, as the water front moves through the HME particle (with concomitant copovidone diffusion into bulk solution), a contiguous particle of amorphous anacetrapib is immediately formed behind the advancing water front. Figures 11 and 12b–f show that this scaffold particle is actually composed of much smaller, aggregated amorphous anacetrapib nanostructures. Given the amorphous anacetrapib solubility data in Table 2 (upper), which shows that even 100 mg/mL copovidone in water provides only 0.001 mg/mL anacetrapib solubility, we cannot rationalize 20% by weight anacetrapib (200 mg/mL) transiently solubilizing and then rapidly precipitating to form these nanostructures. In our view a more plausible construct is that the copovidone dissolution promotes rapid *amorphous phase separation* of the anacetrapib. The phase separation proceeds in three dimensions along the advancing water front moving through the HME particle. Similar rapid phase separation (in less than 10 s) in copovidone/drug films upon dipping the films in water was recently demonstrated by Purohit and Taylor[28] using fluorescent probes.

The scaffold particle formation derives from a "hydrophobic capture" of the amorphous domains formed within each HME particle (Figure 12e,f). That is, at 20% anacetrapib in the HME particle, the number of amorphous domains forming is large enough, and their proximity to each other close enough, that diffusion will lead to collisions of the domains with each other within the few millisecond time scale.[29] Hydrophobic–hydrophobic interactions thus drive rapid domain aggregation to form larger structures (the scaffold particle). The hydrophobic contacts between amorphous domains provide the structural integrity to the scaffold particle and prevent escape of the amorphous domains into the bulk solution, where they would otherwise be detected as "nanoparticles". Sonication, however (Figure 11), quickly breaks apart most of the hydrophobic–hydrophobic domain contacts. Scheme 1 depicts these concepts for a ca. 70 μm 0% TPGS HME particle in water (note in Scheme 1A, the entire HME particle is depicted *after* copovidone exit and subsequent anacetrapib amorphous domain formation).

This simple conceptualization would mean that significantly lower anacetrapib drug loadings in copovidone might avoid such hydrophobic capture by decreasing the spatial density of phase-separated domains forming within the HME particle volume. To this end we manufactured a 2% drug load anacetrapib/98% copovidone HME milled powder. Analysis as in Figure 2 reveals that, with only simple stirring, within several minutes a maximum value of ~65% of the anacetrapib is released to bulk solution as nanoparticles (free anacetrapib amorphous domains). This 65% nanoparticle yield is ca. 30-fold higher than the 20% drug loading nanoparticle yield (<2%, Figure 2). This trend of lower nanoparticle yield at higher drug
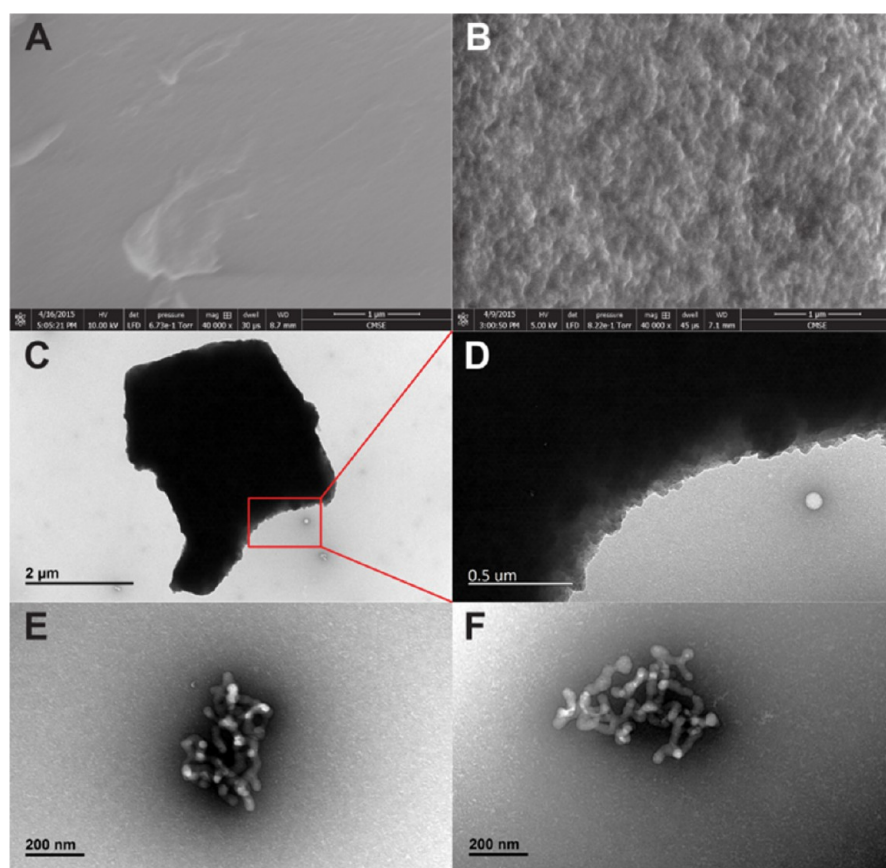
Figure 12. Images A and B are SEM (40,000 magnification) of original 0% TPGS milled HME particle prior to contact with water (A) and after contact with excess water and copovidone exit (B, scale bar 1 μm in images A and B). Image C is a TEM of a several micrometer sized piece of a 0% TPGS scaffold particle isolated from stirred water solution. Image D shows the TEM of the edge region indicated on image C (note scalebars). Images E and F are TEM images of sub-micrometer pieces of 0% TPGS scaffold particles isolated from the same stirred water solutions. Note scalebar is 200 nm in images E and F.

Table 2. Impact of Anacetrapib Solubility by Added TPGS and Copovidone and Relevant Thermal Properties of Anacetrapib

Impact of Anacetrapib Solubility by Added TPGS				
	water	100 mg/mL copovidone	20 mg/mL TPGS	100 mg/mL TPGS
solubility of amorphous anacetrapib (mg/mL)	<0.001	<0.001	0.13	2
Relevant Thermal Properties of Anacetrapib				
thermal properties	melting point (°C)		T_g (°C)	
anacetrapib	72		43	
TPGS	37−41		not detected	

loadings was noted by Taylor[14] and will be discussed further below.

General Effects of TPGS Present in HME Particles: Rapid Adsorption onto Amorphous Anacetrapib Phase-Separated Domain Surfaces and Mitigation of Hydrophobic Capture. An overall consideration of the data obtained above leads us to believe that the presence of TPGS in the HME particles studied (Table 1) does not impact the amorphous phase separation event. Rather, the main impact of TPGS is through rapid TPGS absorption *onto* the amorphous anacetrapib phase separated domain surfaces. While the data in Figure 10 clearly localize significant TPGS on anacetrapib nanoparticle surfaces after nanoparticle release to bulk solution, the TPGS data in Figures 3 and 4 show that all the TPGS is initially sequestered within the 1%, 2%, 3.5%, and 5% TPGS scaffold particles until anacetrapib nanoparticle release (no TPGS accompanies the kinetic profile of the copovidone exit to bulk solution). This data suggests that the amphiphilic nature of TPGS provides for a high affinity for amorphous anacetrapib particle surfaces within the transient scaffold particles, even compared to its own solubility in water. Given the number density of amorphous anacetrapib domains forming, if TPGS were initially in solution "between" these domains, we estimate[30] that it would take on the order of only tens of microseconds for TPGS to diffusionally encounter anacetrapib domains. This is much faster than the anacetrapib–anacetrapib domain diffusional encounter time frame of milliseconds described above; thus TPGS adsorption would occur prior to domain diffusional contact.

At the highest TPGS levels studied here (7.2% and 10% by weight in the HME, Table 1), it is hypothesized that the TPGS is able to rapidly adsorb onto the amorphous anacetrapib domain surfaces at a high enough surface density to mitigate hydrophobic capture entirely. In this regime, the TPGS-coated amorphous domains can immediately diffuse to bulk solution. In our view, the ca. 50−60 nm D_{50} nanoparticle distributions found for the 7.2% and 10% TPGS cases (Figure 5, Table S1) reflect formation (and escape to bulk solution) of the *same* anacetrapib amorphous domain distribution which is hydrophobically captured in the 0% TPGS particle (note the ca. 50

Scheme 1. 0% TPGS HME Particle in Water[a]
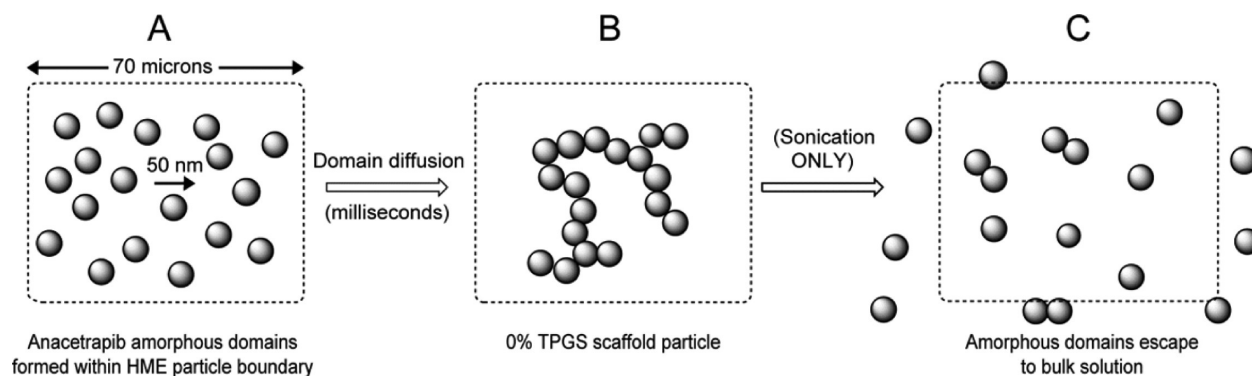
[a](A) Anacetrapib amorphous domain formation within the HME particle volume (dashed line) shown post copovidone exit. (B) Domain diffusion resulting in hydrophobic capture (scaffold particle formation, Figure 12 e,f). (C) Sonication of the scaffold particle to release domain structures (nanoparticles) into bulk solution.

Table 3

	Scaffold Particle Forming Compositions[a]				
% TPGS in HME	equilibration time (min)	no. of TPGS molecules in 50 mg of HME	annealed nanoparticle size (D_{50}, nm)	total nanoparticle SA (Å^2)	SA (Å^2) per TPGS molecule
2.0	25.0	4.0×10^{17}	190	2.4×10^{19}	60
3.5	4.0	7.0×10^{17}	110	4.2×10^{19}	60
5.0	1.0	1.0×10^{18}	77	6.0×10^{19}	60
	Immediate Release of Nanoparticles[b]				
% TPGS in HME	equilibration time (min)	no. of TPGS molecules in 50 mg of HME	nanoparticle size (D_{50}, nm)	nanoparticle SA (Å^2)	enough TPGS to cover at 60 Å^2/ TPGS?
7.2	none (IR)	1.4×10^{18}	55	8.3×10^{19}	yes
10.0	none (IR)	2.0×10^{18}	48	9.6×10^{19}	yes (20% excess)

[a]Calculated total nanoparticle surface area (SA) (Å^2) per TPGS molecule in scaffold particles just prior to release of nanoparticles (upper) to the bulk solution (2%−5% TPGS HME compositions, assumes 50 mg of HME added to water). [b]Comparison of maximum TPGS coverage which can be provided to the 55 and 48 nm nanoparticle populations to the closest packed monolayer possible for TPGS.
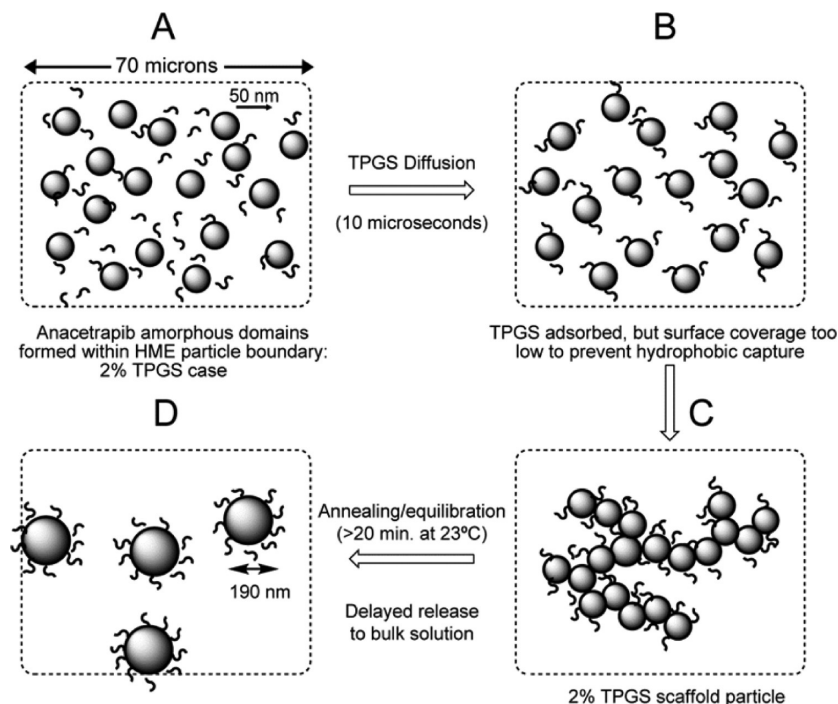
Scheme 2. 7.2 and 10% TPGS HME Particles in Water[a]
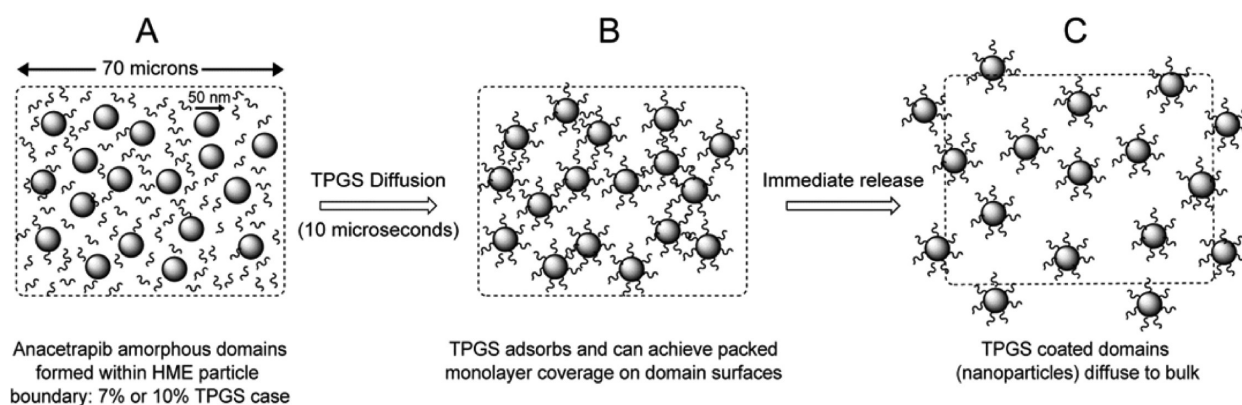
[a](A) Anacetrapib amorphous domain formation post copovidone exit, with TPGS molecules depicted initially dissolved in the water phase. (B) TPGS diffusion to domain surfaces forming essentially best-packed monolayer coverage mitigating hydrophobic capture. (C) Diffusion of the TPGS-coated nanoparticles to bulk solution.

nm domain sub-structures within the 0% TPGS scaffold particle TEM image in Figure 12F).

It is worthwhile to more quantitatively consider the TPGS surface coverage possible in this context. Langmuir trough studies of TPGS[31] have shown that the closest packed TPGS monolayer possible corresponds to a packing density of 60−65 Å^2/TPGS molecule. The lower portion of Table 3 assumes that all the TPGS present in the 7.2% and 10% TPGS HME

compositions is initially adsorbed onto nanoparticle (domain) surfaces. In the 7.2% TPGS case there is just enough TPGS to provide ~60 Å^2/TPGS molecule coverage on the 55 nm D_{50} nanoparticles.[32] The 10% TPGS case has more than enough TPGS to provide the 60−65 Å^2/TPGS molecule coverage (TPGS is in 20% excess). Only these two HME compositions are able to provide enough TPGS to prevent hydrophobic capture of the primary amorphous anacetrapib domain size

Scheme 3. 2% TPGS HME Particle in Water[a]

[a](A) Anacetrapib amorphous domain formation post copovidone exit, with TPGS molecules depicted initially dissolved in the water phase. (B) TPGS diffusion to domain surfaces; only fractional monolayer coverage can occur. (C) Transient hydrophobic capture. (D) Nanoparticle growth (annealing/equilibration) driving TPGS to closest packed monolayer coverage and concomitant nanoparticle release to bulk solution.

distribution formed. Scheme 2 depicts the impact of 7.2−10% TPGS in the HME particle and should be compared to Scheme 1 (note that Scheme 2A depicts the entire HME particle after copovidone exit and subsequent anacetrapib amorphous domain formation, yet before TPGS diffusion).

The 2%, 3.5%, and 5% TPGS HME Particles: Initial Scaffold Particle Formation and Subsequent Amorphous Domain Annealing. Table 3 and the discussion above highlight that the 2%−5% TPGS compositions cannot provide enough TPGS to achieve the 60−65 Å^2/TPGS molecule maximum coverage of the ca. 50−60 nm D_{50} amorphous domain distribution initially formed. These TPGS surface coverage values are apparently insufficient to prevent a transient hydrophobic capture, and scaffold particle formation occurs (Figure 8 e,f for the 2% TPGS HME particle, Figure 9 d,e for the 5% TPGS case). Scheme 3A−C depicts this process (note that Scheme 3A depicts the entire HME particle after copovidone exit and subsequent anacetrapib amorphous domain formation, yet before TPGS diffusion). The 5%, 3.5%, and 2% TPGS HME scaffold particles exist in stirred solutions (23 °C) for 1 min, ∼3 min, and ∼25 min, respectively, before they begin to spontaneously release TPGS-coated amorphous anacetrapib nanoparticles (Figure 3, lower, Figure 4, and Table 3).

The sizes of the nanoparticles which are subsequently released after these 1−25 min "delay periods" are remarkable, in that they are all significantly *larger* than the 50−60 nm D_{50} amorphous anacetrapib domain size distribution initially being formed from the copovidone exit. We have taken the 2%−5% TPGS nanoparticle samples as measured in Figure 5 and sonicated them. The D_{50} values do not change (data not shown), which demonstrates that these larger nanoparticles are not simply aggregates of smaller particles. Further, for the 2%

TPGS scaffold particle we find that sonication over the 3−20 min time period—prior to spontaneous release of nanoparticles—gives D_{50} values which steadily *increase* from ∼70 nm at 3 min to near 170 nm at 20 min (data not shown).

Our rationale of these very interesting phenomena follows. The anacetrapib domain and TPGS distributions depicted in Scheme 3C derive from the kinetic effects described, and their distributions may not be at thermal equilibrium. The delay periods noted above we believe are thermal equilibration periods during which the anacetrapib domains undergo annealing or coalescence as depicted in Scheme 3D. The top portion of Table 3 calculates the TPGS surface coverages that are being achieved by this annealing in the 2%−5% TPGS cases, using the annealed nanoparticle size[32] (size released to bulk solution after spontaneous release). Remarkably, Table 3 shows in each case that the amorphous domain size distribution which initially forms has been annealed such that all the TPGS present is involved in the same maximum 60 Å^2/TPGS molecule surface coverage of anacetrapib nanoparticles. In this limit, the total surface area of the nanoparticles released responds "linearly" to the % TPGS in the extrudate. For a fixed mass of particles each with a radius r, the total surface area of the ensemble of particles changes as $1/r$ as r is varied (the ensemble surface area will be reduced 2-fold if the radius is doubled, for example). The lower portion of Figure 13 plots $1/r$ against the % TPGS present in the extrudate. The 2−5% TPGS data is highly linear and gives a Y-axis intercept near zero (very large nanoparticle size as the % TPGS in the extrudate approaches zero). Once TPGS surface coverage approaches 60 Å^2/TPGS molecule, all hydrophobic contacts between anacetrapib solids are lost and the scaffold particle spontaneously releases TPGS coated nanoparticles to solution. Note that, in terms of energy minimizations, the process we are
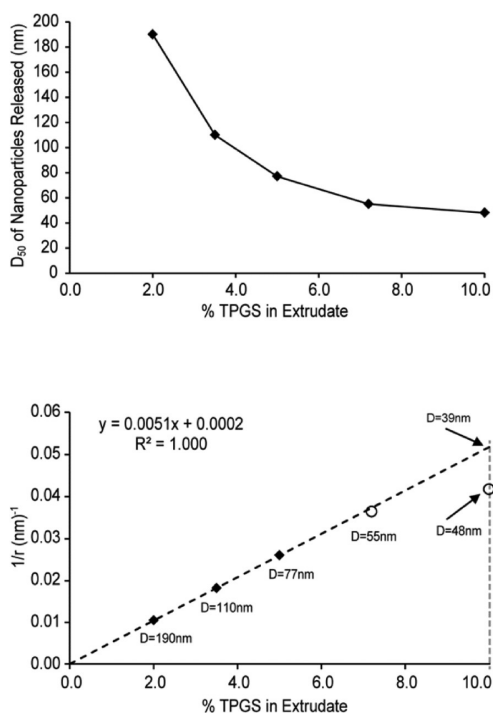
Figure 13. Upper: Plot of D_{50} for spontaneously released nanoparticles (Table S1) versus % TPGS in the extrudate. Lower: Same plot where D_{50} is expressed as $1/r$. The 7.2% and 10% TPGS data points were not included in the linear fit shown since there is no annealing process (no scaffold particle formation).

proposing in Scheme 3C,D has some analogies to how oil droplets and surfactants interact to form stable emulsions[33−35] in water. We note that it is possible that this annealing behavior (Scheme 3C,D) may be specific to anacetrapib and TPGS.

The 1% TPGS HME Case. In the 1% TPGS case, similar quantitative TPGS adsorption onto the primary anacetrapib amorphous domains occurs (Figure 4), and again the low TPGS surface coverage allows hydrophobic capture. The TPGS can only slowly diffuse out of the 1% TPGS HME scaffold particle structure (Figure 4). We separated discussion of this case from the 2%−5% TPGS cases only in that no annealing process and subsequent spontaneous nanoparticle release are observed over the conditions of our primary experiment (2 h stirring at 23 °C, Figure 2).

Role of Anacetrapib T_g in Relation to Experimental Temperature. The melting point of amorphous anacetrapib is 72 °C, and the T_g is 43 °C (Table 2). Thus, anacetrapib is in a glassy state at our 23 °C dissolution conditions.[36] We have surveyed the dissolution behaviors of the compositions in Table 1 between 23 and 43 °C to broaden the observations here across the glass and supercooled liquid states. Three general observations describe these findings. First, the behaviors of the 0%, 7.2%, and 10% TPGS compositions remain unchanged; the nanoparticle yield for the 0% TPGS is very low, and the same nanoparticle sizes are formed (again rapidly and in high yield) for the 7.2% and 10% TPGS cases as shown in Table S1 for the 23 °C case. Thus, Schemes 1 and 2 apply similarly throughout the 23−43 °C range. Second, the equilibration periods (listed in Table 3) for the 2%−5% TPGS HME cases shorten significantly as the temperature of the experiment is increased to 43 °C; however the nanoparticle sizes spontaneously released are identical to those listed in Table S1 for the 23

°C experiment. This general result is consistent with a higher mobility of the "liquid" anacetrapib at 43 °C to promote a more rapid domain annealing, which we view as rate-limiting in the equilibration process. Finally, the 1% TPGS composition will spontaneously release nanoparticles at later times at the elevated temperatures studied (about 4 h at 43 °C will lead to over 90% nanoparticle yield). Consistent with the right-hand column in Table 3, these nanoparticles have a D_{50} value over 350 nm.

Generality of Amorphous Phase Separation and Scaffold Particle Formation in Other Copovidone/Drug ASD Systems. As described above, we view all the anacetrapib nanoparticles found here to have their origins from copovidone dissolution and rapid amorphous anacetrapib phase separation occurring within each HME particle. Previous literature reports suggest[14] or imply[6,12,16] that amorphous nanoparticle formation in ASDs occurs by a precipitation event from a region of very highly supersaturated dissolved drug "near" or "local" to the dissolving ASD particle[14] (this supersaturation would be with respect to the *amorphous* solubility limit if amorphous nanoparticles are being formed). In this view most of the drug present in the ASD particle, at some point during dissolution of the particle, is thought to be transiently dissolved in this local volume of solution. If we presume that this "local volume" of solution might be thought of as the ASD particle's diffusion layer, then the amorphous phase separation construct described here provides a marked contrast. In the current case we would expect ASD diffusion layers to be only saturated with the amorphous drug as phase separation/domain formation proceeds. Scaffold particle formation can thus occur with only a minor fraction of the drug in the ASD particle ever being "solubilized." It is likely these two limits are best framed as being on opposite ends of a "continuum" as depicted and described in Scheme 4. It strikes us that drug solubility and drug loading will largely determine where on the continuum one resides.

Scheme 4. Conceptual Continuum of Behaviors of Copovidone-Based ASD Particles during Dissolution in Water[a]
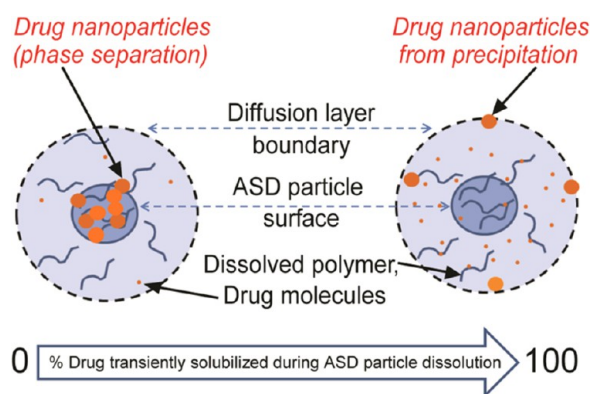
[a]Scheme assumes no surfactant in particle, 10−50% drug loading, and the drug has low crystallization potential. The left-hand side depicts rapid phase separation and hydrophobic capture of amorphous drug domains as described here for anacetrapib (lowest solubility drugs). The right-hand side depicts drug nanoparticle origins from precipitation within very highly supersaturated ASD particle diffusion layers (higher solubility drugs).

In our experience, copovidone has limited affinity for low solubility compounds and poor solubilizing power for drug molecules that are being processed into ASDs (solubility data in Table 2 is typical). These properties, along with the very high copovidone water solubility, in combination with very poorly soluble drug candidates might generally promote the rapid amorphous phase separation route shown on the left-hand side of Scheme 4. In our laboratory we have seen rapid copovidone exit from ASDs for numerous drug substances, all of which have higher water solubility than the present anacetrapib case. We have observed similar hydrophobic capture events (although with a varying extent or degree of hydrophobic capture) across a wide range of generally low solubility drug substances.

The drug loading effect on nanoparticle release to bulk solution we have noted here for 2% and 20% anacetrapib (reviewed in the upper 2 lines of Table 4) is explained in the

Table 4. Nanoparticle Yields from Various Copovidone/Drug/TPGS Compositions, Showing the Ability of TPGS To Mitigate against Hydrophobic Capture of Amorphous Anacetrapib Domains

HME composition (copovidone/drug/TPGS)	nanoparticle yield (% mass sub 1 μm)
98/2/0	65
80/20/0	<2
70−78/20/10−2	>90
55/40/5	∼60

current context by more pronounced hydrophobic capture events as drug loading increases (higher drug loading gives increased spatial densities of the amorphous domains initially forming). This same effect of lower sub-micrometer particle yields at higher drug loadings was noted by Taylor,[14] who interpreted their data in the context of previous work by Simonelli[37] and Corrigan[38] and later reviewed by Craig.[21] The lower nanoparticle yield (at higher drug loading) was explained by formation of a drug-rich layer developing at the dissolving ASD particle diffusion front. In the context of Scheme 4 (right-hand side) the amorphous drug-rich layer serves to reduce the degree of supersaturation (lowering it to near the drug amorphous solubility value) thus removing the driving force for amorphous nanoparticle formation.[14] Given our observations here we would offer the possibility (particularly for the copovidone-based ASDs[14]) that the drug-rich layer itself was already the result of amorphous domain (nanoparticle) formation and subsequent hydrophobic capture, at the higher 50% drug loading.

Commonly used cellulosic polymers in ASDs (such as HPMCAS or HPMC) may result in somewhat different behaviors than the copovidone-based systems discussed here (detailed studies of these systems are beyond the scope of the current work). HPMCAS, for example, has a much stronger affinity for low solubility drug molecules than copovidone, and has water solubility of only ca. 5 mg/mL (copovidone is soluble at several hundred mg/mL). As a result the drug and HPMCAS polymer tend to dissolve out of the ASD particle at more similar rates, and the scaffold particle formation we have described here is less likely. However, at the surface of the HPMCAS ASD particle, similar drug phase separation[6] and subsequent domain hydrophobic capture to produce "local drug enrichment" is possible.

Surfactant Use in Copovidone ASDs: Maximizing Nanoparticle Yields and Drug Loadings. This work focuses on the mechanism of amorphous nanoparticle formation in copovidone-based ASDs using anacetrapib as an example. Investigation into what type of ASD polymer systems (for example, cellulosic or PVP-based) might actually provide for maximum anacetrapib human exposures is not the focus of the current work. However, in general if the recrystallization potential of a drug is very low, then highly efficient amorphous nanoparticle formation from a copovidone-based ASD particle offers an excellent route to maximizing dissolution rate at any given amorphous solubility value. In this context it is worth noting that the 0% TPGS scaffold particles described here remain intact (very little nanoparticle release to bulk solution) even with several hours of 150 rpm stirring in fasted simulated intestinal fluids at 23 or 37 °C. Thus, we would expect the in vivo dissolution rate from the 0% TPGS scaffold particle to be slower than if all the amorphous domains had been released to bulk solution.

This work brings into clear view an important role that surfactants may play in copovidone or PVP ASD systems: mitigating hydrophobic capture by amorphous domain passivation. This allows the nanoparticles to freely diffuse into bulk solution where they can provide maximum dissolution rates. The view of nanoparticle formation depicted on the right-hand side of Scheme 4, in contrast, casts surfactant largely as a solubilizing agent to promote local supersaturation (thus enhancing subsequent nanoparticle precipitation). Depending on where the copovidone-based ASD formulation sits on the continuum depicted in Scheme 4, these two different properties of surfactants may be differentially important in impacting nanoparticle yields.

While there are several reports in the literature around increasing dissolution rates of copovidone-based ASDs by use of TPGS[31,39] or other surfactants,[16,17,20,40,41] none to our knowledge have examined such behavior in terms of measured increases in nanoparticle formation yields. In our view this highlights that the hydrophobic capture—scaffold particle formation limit described here is not currently appreciated by many pharmaceutical scientists. Table 4 offers an excellent view of the possibilities demonstrated within the context of the copovidone—TPGS—anacetrapib ternary composition examined here. The first three rows of Table 4 compile data already described above, while we now discuss the 40% anacetrapib drug load data. Inclusion of TPGS even at 5% still allows ∼65% of the anacetrapib in the 40% drug load HME particle to escape to bulk solution as sub-micrometer particles. Table 4 and a consideration of Scheme 4 highlight that careful and judicious choice of surfactant in copovidone-based (and likely PVP-based) ASD systems should be undertaken, if the optimal nanoparticle yield at the highest possible drug loading is a desired outcome.

Finally, it is worth noting that the behaviors we are describing here also do not appear to depend on whether or not the ASD particle is made by the HME or the SD route. To this point we note here that we have manufactured the same 0%, 2%, 3.5%, and 10% TPGS HME ASD compositions (Table 1) by the SD route and carried out identical dissolution studies as described. Similar scaffold particle formation, TPGS passivation, and nanoparticle release characteristics and sizes are observed for the SD ASD particles. This suggests that different process technology routes (SD versus HME) of the same copovidone-based ASD composition will give similar

dissolution behaviors, as compared to different ASD particle compositions.

CONCLUSIONS

A systematic study of a copovidone-based HME of anacetrapib as a function of added TPGS content in the HME particle is reported. The data enable a holistic mechanistic rationalization of nanoparticle formation and release (or lack of release) across the entire 0%−10% TPGS range. The origin of nanoparticle formation is an amorphous anacetrapib phase separation, driven by rapid copovidone dissolution from the HME particle. In the current case, without TPGS in the HME particle, the amorphous domains undergo hydrophobic capture and form a contiguous scaffold particle. At the 7.2% and 10% TPGS levels, TPGS adsorption can passivate the hydrophobic amorphous domains prior to hydrophobic capture and the amorphous domains diffuse to bulk solution as nanoparticles. In the 2%−5% TPGS range, the TPGS still adsorbs rapidly onto the amorphous anacetrapib domains, but cannot prevent their initial hydrophobic capture. However, during an equilibration period, the domain surface area is reduced until the available TPGS can cover the anacetrapib nanoparticle surface area at a packing density of about 60 Å^2/TPGS molecule. At this point the nanoparticles can be released from the scaffold particle to bulk solution. The phase separation aspects of the nanoparticle formation described here, in our view, are likely applicable to other copovidone/drug ASD systems studied in the literature, whether or not they contain surfactants in the ASD particles. The work here highlights the important role that surfactant and drug loading play in increasing nanoparticle yields and extending the useful drug loading ranges that might be utilized in copovidone- or PVP-based HME or SD ASDs.

ASSOCIATED CONTENT

Ⓢ Supporting Information

The Supporting Information is available free of charge on the ACS Publications website at DOI: 10.1021/acs.molpharmaceut.5b00863.

Tables of D_{50}, PSD width, and % TPGS values (PDF)

AUTHOR INFORMATION

Corresponding Author
*Tel: 215-652-4214. E-mail: paul_harmon@merck.com.
Notes
The authors declare no competing financial interest.

ACKNOWLEDGMENTS

REFERENCES

(1) Chen, X. Q.; Antman, M. D.; Gesenberg, C.; Gudmundsson, O. S. Discovery Pharmaceutics - Challenges and Opportunities. *AAPS J.* **2006**, *8*, E402−E408.

(2) Merisko-Liversidge, E. M.; Liversidge, G. G. Drug Nanoparticles: Formulating Poorly Soluble Compounds. *Toxicol. Pathol.* **2008**, *36*, 43−48.

(3) Patel, D.; Sawant, K. K. Self Micro-emulsifying Drug Delivery System: Formulation Development and Biopharmaceutical Evaluation of Lipophilic Drugs. *Curr. Drug Delivery* **2009**, *6*, 419−424.

(4) Kyatanwar, A. U.; Jadhav, K. R.; Kadam, V. J. Self Micro-emulsifying Drug Delivery System (SMEDDS): Review. *J. Pharmacy Res.* **2010**, *3* (1), 75−83.

(5) Neervannan, S. Preclinical Formulations for Discovery and Toxicology: Physiochemical Challenges. *Expert Opin. Drug Metab. Toxicol.* **2006**, *2*, 715−731.

(6) Friesen, D. T.; Shanker, R.; Crew, M.; Smithey, D. T.; Curatolo, W.; Nightingale, J. Hydroxypropyl Methylcellulose Acetate Succinate-Based Spray-Dried Dispersions: An Overview. *Mol. Pharmaceutics* **2008**, *5* (6), 1003−1019.

(7) Breitenbach, J. Melt Extrusion: From Process to Drug Delivery Technology. *Eur. J. Pharm. Biopharm.* **2002**, *54* (2), 107−117.

(8) Leuner, C.; Dressman, J. Improving Drug Solubility for Oral Delivery Using Solid Dispersions. *Eur. J. Pharm. Biopharm.* **2000**, *50* (1), 47−60.

(9) Murdande, S. B.; Pikal, M. J.; Shanker, R. M.; Bogner, R. H. Solubility Advantage of Amorphous Pharmaceuticals: I. A Thermodynamic Analysis. *J. Pharm. Sci.* **2010**, *99* (3), 1254−1264.

(10) Vasconcelos, T.; Sarmento, B.; Costa, P. Solid Dispersions as Strategy to Improve Oral Bioavailability of Poor Water Soluble Drugs. *Drug Discovery Today* **2007**, *12* (23−24), 1068−1075.

(11) Bikiaris, D. N. Solid dispersions, Part I: Recent Evolutions and Future Opportunities in Manufacturing Methods for Dissolution Rate Enhancement of Poorly Water-Soluble Drugs. *Expert Opin. Drug Delivery* **2011**, *8* (11), 1501−1519.

(12) Huang, Y.; Dai, W. Fundamental Aspects of Solid Dispersion Technology for Poorly Soluble Drugs. *Acta Pharm. Sin. B* **2014**, *4* (1), 18−25.

(13) Alonzo, D. E.; Zhang, G. G.; Zhou, D.; Gao, Y.; Taylor, L. S. Understanding the Behavior of Amorphous Pharmaceutical Systems during Dissolution. *Pharm. Res.* **2010**, *27* (4), 608−618.

(14) Alonzo, D. E.; Gao, Y.; Zhou, D.; Mo, H.; Zhang, G. G.; Taylor, L. S. Dissolution and Precipitation Behavior of Amorphous Solid Dispersions. *J. Pharm. Sci.* **2011**, *100* (8), 3316−3331.

(15) Raina, S. A.; Zhang, G. G.; Alonzo, D. E.; Wu, J.; Zhu, D.; Catron, N. D.; Gao, Y.; Taylor, L. S. Enhancements and Limits in Drug Membrane Transport Using Supersaturated Solutions of Poorly Water Soluble Drugs. *J. Pharm. Sci.* **2014**, *103* (9), 2736−2748.

(16) Kanaujia, P.; Lau, G.; Ng, W. K.; Widjaja, E.; Hanefeld, A.; Fischbach, M.; Maio, M.; Tan, R. B. Nanoparticle Formation and Growth During In Vitro Dissolution of Ketoconazole Solid Dispersion. *J. Pharm. Sci.* **2011**, *100* (7), 2876−2885.

(17) Frank, K. J.; Westedt, U.; Rosenblatt, K. M.; Hoelig, P.; Rosenberg, J.; Maegerlein, M.; Fricker, G.; Brandl, M. What Is the Mechanism Behind Increased Permeation Rate of a Poorly Soluble Drug from Aqueous Dispersions of an Amorphous Solid Dispersion? *J. Pharm. Sci.* **2014**, *103* (6), 1779−1786.

(18) Kanzer, J.; Hupfeld, S.; Vasskog, T.; Tho, I.; Hoelig, P.; Maegerlein, M.; Fricker, G.; Brandl, M. In Situ Formation of Nanoparticles Upon Dispersion of Melt Extrudate Formulations in Aqueous Medium Assessed by Asymmetrical Flow Field-Flow Fractionation. *J. Pharm. Biomed. Anal.* **2010**, *53* (3), 359−365.

(19) Ilevbare, G. A.; Taylor, L. S. Liquid-Liquid Phase Separation in Highly Supersaturated Aqueous Solutions of Poorly Water-Soluble Drugs: Implications for Solubility Enhancing Formulations. *Cryst. Growth Des.* **2013**, *13* (4), 1497−1509.

(20) Frank, K. J.; Westedt, U.; Rosenblatt, K. M.; Hoelig, P.; Rosenberg, J.; Maegerlein, M.; Fricker, G.; Brandl, M. The Amorphous Solid Dispersion of the Poorly Soluble ABT-102 Forms Nano/microparticulate Structures in Aqueous Medium: impact on Solubility. *Int. J. Nanomed.* **2012**, *7*, 5757−5768.

(21) Craig, D. Q. M. The Mechanisms of Drug Release From Solid Dispersions in Water-Soluble Polymers. *Int. J. Pharm.* **2002**, *231* (2), 131−144.

(22) Friedrich, H.; Frederik, P. M.; de With, G.; Sommerdijk, N. A. Imaging of Self-Assembled Structures: Interpretation of TEM and Cryo-TEM Images. *Angew. Chem., Int. Ed.* **2010**, *49* (43), 7850−7858.

(23) Cheng, D.; Mitchell, D. R. G.; Shieh, D.-B.; Braet, F. Practical Considerations in the Successful Preparation of Specimens for Thin-Film Cryo-Transmission Electron Microscopy. In *Current Microscopy Contributions to Advances in Science and Technology*, Vol. 2; Mendez-Vilas, A., Ed.; Formatex Research Center: Badajoz, 2012; pp 880−890.

(24) Margulis, K.; Magdassi, S.; Lee, H. S.; Macosko, C. W. Formation of Curcumin Nanoparticles by Flash Nanoprecipitation From Emulsions. *J. Colloid Interface Sci.* **2014**, *434*, 65−70.

(25) Hilhorst, J.; Meester, V.; Groeneveld, E.; Dhont, J. K.; Lekkerkerker, H. N. Structure and Rheology of Mixed Suspensions of Montmorillonite and Silica Nanoparticles. *J. Phys. Chem. B* **2014**, *118* (40), 11816−11825.

(26) Higher SLS levels were not utilized to keep the below the SLS critical micelle concentration in order to minimize solubilization of the anacetrapib nanoparticles.

(27) Assuming 60% associated TPGS and a 50 nm (diameter) anacetrapib particle, that corresponds to 6 mg of TPGS associated per 20 mg of anacetrapib. Given that the TPGS must have a density more like the vitrified ice of around 0.95 (image, Figure 6) and using a density of 1.3 g/cm^3 for the anacetrapib, the 6 mg of TPGS would require an annular volume which corresponds to a 3 nm thick layer around each 50 nm particle (6 nm spacing between adjacent particles).

(28) Purohit, H. S.; Taylor, L. S. Phase Separation Kinetics in Amorphous Solid Dispersions Upon Exposure to Water. *Mol. Pharmaceutics* **2015**, *12* (5), 1623−1635.

(29) Anacetrapib domains must fill about 15% of the original HME particle volume (20% drug load, assuming a density of 1.3 g/cm^3). Assuming a domain size of 70 nm and a uniformly spaced domain distribution, the outer surface of each particle will be about 1 particle diameter from adjacent domains. The domain diffusion coefficient can be estimated at 1×10^{-8} cm^2/s, giving a diffusion time of several milliseconds to diffuse 70 nm.

(30) A diffusion coefficient of about 3×10^{-6} cm^2/s for TPGS can be estimated. In 10 μs TPGS would diffuse around 70 nm (roughly the amorphous domain spacing).

(31) Mu, L.; Seow, P. H. Application of TPGS in Polymeric Nanoparticulate Drug Delivery System. *Colloids Surf., B* **2006**, *47* (1), 90−97.

(32) The D_{50} is used to represent all nanoparticles. A density of 1.3 g/cm^3 is assumed. Total nanoparticle surface area is calculated and divided by the total number of TPGS molecules present.

(33) Capek, I. Degradation of Kinetically-Stable o/w Emulsions. *Adv. Colloid Interface Sci.* **2004**, *107* (2−3), 125−155.

(34) Pichot, R.; Spyropoulos, F.; Norton, I. O/W Emulsions Stabilized by both Low Molecular Weight Surfactants and Colloidal Particles: The Effect of Surfactant Type and Concentration. *J. Colloid Interface Sci.* **2010**, *352* (1), 128−135.

(35) Henry, J. V.; Fryer, P. J.; Frith, W. J.; Norton, I. T. Emulsification Mechanism and Storage Instabilities of Hydrocarbon-in-Water Sub-Micron Emulsions Stabilised with Tweens (20 and 80), Brij 96v and Sucrose Monoesters. *J. Colloid Interface Sci.* **2009**, *338* (1), 201−206.

(36) Amorphous anacetrapib has very low water content even at 95% RH (about 0.05%). Thus we expect the T_g reported in Table 4 to be representative of amorphous anacetrapib nanoparticles in water.

(37) Simonelli, A. P.; Mehta, S. C.; Higuchi, W. I. Dissolution Rates of High Energy Polyvinylpyrrolidone (PVP)-Sulfathiazole Coprecipitates. *J. Pharm. Sci.* **1969**, *58* (5), 538−549.

(38) Corrigan, O. I. Mechanisms of Dissolution of Fast Release Solid Dispersions. *Drug Dev. Ind. Pharm.* **1985**, *11* (2−3), 697−724.

(39) Sotthivirat, S.; McKelvey, C.; Moser, J.; Rege, B.; Xu, W.; Zhang, D. Development of Amorphous Solid Dispersion Formulations of a Poorly Water-Soluble Drug, MK-0364. *Int. J. Pharm.* **2013**, *452* (1−2), 73−81.

(40) Ghebremeskel, A. N.; Vemavarapu, C.; Lodaya, M. Use of Surfactants as Plasticizers in Preparing Solid Dispersions of Poorly Soluble API: Stability Testing of Selected Solid Dispersions. *Pharm. Res.* **2006**, *23* (8), 1928−1936.

(41) Ghebremeskel, A. N.; Vemavarapu, C.; Lodaya, M. Use of Surfactants as Plasticizers in Preparing Solid Dispersions of Poorly Soluble API: Selection of Polymer-Surfactant Combinations Using Solubility Parameters and Testing the Processability. *Int. J. Pharm.* **2007**, *328* (2), 119−129.